

Detections of the 2175 Å Dust Feature at $1.4 \lesssim z \lesssim 1.5$ from the Sloan Digital Sky Survey

Junfeng Wang,¹ Patrick B. Hall,² Jian Ge,¹ Aigen Li,³ and Donald P. Schneider¹

ABSTRACT

The strongest spectroscopic dust extinction feature in the Milky Way, the broad absorption bump at 2175 Å, is generally believed to be caused by aromatic carbonaceous materials – very likely a mixture of Polycyclic Aromatic Hydrocarbon (PAH) molecules, the most abundant and widespread organic molecules in the Milky Way galaxy. In this paper we report identifications of this absorption feature in three galaxies at $1.4 \lesssim z \lesssim 1.5$ which produce intervening Mg II absorption toward quasars discovered by the Sloan Digital Sky Survey (SDSS). The observed spectra can be fit using Galactic-type extinction laws, characterized by parameters $[R_V, E(B - V)] \simeq [0.7, 0.14], [1.9, 0.13],$ and $[5.5, 0.23]$, respectively, where $R_V \equiv A_V/E(B - V)$ is the total-to-selective extinction ratio, $E(B - V) \equiv A_B - A_V$ is the color-excess. These discoveries imply that the dust in these distant quasar absorption systems is similar in composition to that of Milky Way, but with a range of different grain size distributions. The presence of complex aromatic hydrocarbon molecules in such distant galaxies is important for both astrophysical and astrobiological investigations.

Subject headings: quasars: general, absorption lines–dust, extinction–individual (SDSS J144612.98+035154.4; SDSS J145907.19+002401.2; SDSS J012147.73+002718.7)

1. Introduction

The space between the stars of the Galaxy and external galaxies is filled with gaseous ions, atoms, molecules and tiny dust grains. These interstellar grains, spanning a wide

¹Department of Astronomy & Astrophysics, The Pennsylvania State University, 525 Davey Lab, University Park, PA 16802; jwang@astro.psu.edu, jian@astro.psu.edu, dps@astro.psu.edu

²Princeton University Observatory, Princeton, NJ08544-1001; pathall@astro.princeton.edu

³Steward Observatory, and Lunar and Planetary Laboratory, University of Arizona, Tucson, AZ 85721; agli@lpl.arizona.edu

range of sizes from a few angstroms to a few micrometers, are important for the evolution of galaxies, the formation of stars and planetary systems. So far, one of the most best-studied properties of interstellar dust is its obscuration of starlight. The size and composition of interstellar dust are mainly inferred from, respectively, the extinction curve and its spectral features. The strongest spectroscopic interstellar extinction feature in the Galaxy is the broad 2175 Å absorption bump. This feature was first detected by the Aerobee rocket observations (Stecher 1965). In this work we report the detection of the 2175 Å dust extinction bump from individual intervening absorption systems in the spectra of three Sloan Digital Sky Survey (SDSS; York et al. 2000) quasars.

The review of Draine (2003) provides an excellent summary of the properties of the 2175 Å dust extinction bump and theoretical constraints on its carrier. This feature is seen in extinction curves along lines of sight in the Milky Way (MW), the Large Magellanic Cloud (LMC), and some regions of the Small Magellanic Cloud (SMC). Extinction curves in the SMC bar region lack the 2175 Å feature. The central wavelength of the feature varies by only $\pm 0.46\%$ (2σ) around 2175 Å, while its FWHM varies by $\pm 12\%$ (2σ) around 469 Å. Given its substantial band strength, the carrier responsible for the feature must contain at least one of the most abundant elements C, O, Mg, Si or Fe. Although the exact carrier is unknown, Draine (2003) states that “it now seems likely that some form of graphitic carbon is responsible”, most likely polycyclic aromatic hydrocarbons (PAHs; Joblin, Leger, & Martin 1992; Li & Draine 2001; Draine 2003 and references within).

Several previous detections have been reported of the observed 2175 Å feature in distant galaxies using quasar spectra. Pitman, Clayton, & Gordon (2000) presented a good summary of the state of the field as of three years ago, and ruled out several reported detections, which will not be discussed here.

The highest redshift 2175 Å bump observation to date is that of Vernet et al. (2001), who claimed a probable detection in a composite spectrum of radio galaxies at $z \sim 2.5$, although they acknowledged that the detection is difficult to confirm due to the low signal-to-noise ratio (SNR) and blending with Fe II emission at $\lambda > 2300$ Å. Additionally, the dust responsible for the feature does not appear to be located in the host galaxies proper, but rather in the narrow emission-line regions of these radio galaxies where the physical conditions may be quite different, perhaps leading to different carriers for the bump.

The only previous detection of this feature from an individual intervening absorption system was that of Cohen et al. (1999), who detected the 2175 Å feature in a damped Ly α absorber at redshift $z = 0.524$ toward the BL Lac object AO 0235+164 at $z = 0.94$. They found a lower dust-to-gas ratio than in the Galaxy and mentioned that the 2175 Å feature

“suggests there are differences from the average Galactic curve.”¹

Such differences appear to be rather common when the 2175 Å feature is detected with data of sufficient quality to model the extinction curve involved. Malhotra (1997) detected the 2175 Å feature in the composite absorption spectrum of 96 intervening Mg II absorption systems at redshifts $0.2 < z < 2.2$. The strength of the feature was roughly consistent with a standard Galactic dust-to-gas ratio. Falco et al. (1999) reported detections in several $z \lesssim 1$ galaxies responsible for the gravitational lensing of background quasars. Many of the estimated extinction curves do not match the standard $R_V = 3.1$ Galactic curve (e.g., $R_V = 7.2 \pm 0.1$ was found for a $z_l = 0.68$ spiral galaxy). Toft, Hjorth, & Burud (2000) detected the 2175 Å feature from the lensing galaxy of B 1152+199 at $z = 0.44$ and fitted its extinction curve by a Galactic-type extinction law with $1.3 \lesssim R_V \lesssim 2.1$ and $0.9 \lesssim E(B-V) \lesssim 1.1$. Motta et al. (2002) detected a strong 2175 Å bump in a lensing galaxy at $z = 0.83$. Their data are well fitted by a standard $R_V = 2.1 \pm 0.9$ Galactic extinction curve, leading them to suggest that the lens galaxy of SBS 0909+532 contains dust like that of the Galaxy. Wucknitz et al. (2003) may have marginally detected the 2175 Å feature in a lensing galaxy (later identified with a damped Ly α absorber) at $z = 0.93$. They found that using extinction curves with a significant 2175 Å bump reproduces the data better than curves without this feature. Recently Muñoz et al. (2004) reported that the dust in the $z_l = 0.68$ lens galaxy of B 0218+357 shows the 2175 Å bump but produces a very flat ultraviolet extinction curve with $R_V = 12 \pm 2$.

Given the range of extinction curves found in these extragalactic systems, large and well-selected samples extending to higher redshifts are needed to characterize the diversity and evolution of dust properties in the early universe. As a step towards this goal, we present the 2175 Å feature identified in three individual intervening absorption systems in the spectra of three SDSS quasars.

2. Data

One of the goals of the SDSS is to obtain spectra for $\sim 10^5$ quasars to $i = 19.1$ ($i = 20.2$ for $z > 3$ candidates), in addition to the $\sim 10^6$ galaxies that comprise the bulk of the spectroscopic targets (Strauss et al. 2002; Blanton et al. 2003). From astrometrically calibrated drift-scanned imaging data (Gunn et al. 1998; Pier et al. 2003) on the SDSS *ugriz* system (Fukugita et al. 1996), quasar candidates are selected primarily using color

¹The average Galactic curve is parameterized by $R_V = 3.1$, where $R_V \equiv A_V/E(B-V)$ is the ratio of total to selective extinction and $E(B-V) \equiv A(B) - A(V)$ is the color excess.

criteria designed to target objects whose broad-band colors are different from those of normal stars and galaxies (Richards et al. 2002). Due to these inclusive criteria, the selection of candidates using i band magnitudes rather than blue magnitudes which are more affected by absorption and reddening, and its area and depth, the SDSS can reveal quasars with previously rarely seen properties. Relevant instrumental and observational details of the SDSS Data Release One (hereafter DR1) can be found in Abazajian et al. (2003). The DR1 spectra distributed by the SDSS cover approximately 3800–9200 Å and have been sky subtracted, wavelength calibrated to the heliocentric frame, corrected for telluric absorption and also for Galactic extinction. One of us (P. B. H.) carried out a visual inspection of the SDSS spectra of the $\simeq 6350$ DR1 quasars with $z \geq 1.6$ (Schneider et al. 2003). The goal was to identify examples of unusual quasar subtypes (primarily broad absorption line quasars, nitrogen-strong quasars, and dust-reddened quasars) for later comparison with the results of automated searches. This inspection uncovered several quasars with a possible 2175 Å signature, the most convincing three of which are SDSS J145907.19+002401.2, SDSS J144612.98+035154.4 and SDSS J012147.73+002718.7 (hereafter simply SDSS J1459+0024, SDSS J1446+0351 and SDSS J0121+0027).

3. Fitting and Results

The spectral index α redward of the Lyman α emission line — defined by fitting a power-law $f_\lambda \propto \lambda^{-(\alpha+2)}$ to the continuum — confirms possible reddening in these quasar spectra when compared to the composite quasar spectrum generated using a homogeneous data set of more than 2200 SDSS quasar spectra (Vanden Berk et al. 2001). As shown in Figure 1, compared to that composite’s mean spectral index of ≈ -0.46 , SDSS J1446+0351 has $\alpha \approx -1.93$, SDSS J1459+0024 has $\alpha \approx -1.91$, and SDSS J0121+0027 has $\alpha \approx -1.27$, all suggesting either unusually red intrinsic continua or heavily dust-reddened spectra. We synthesized g , r , and i magnitudes from each spectrum independently and compared these values to the SDSS photometric measurements; this comparison demonstrated that the spectrophotometric calibrations of the spectra are accurate.

Since quasars have a range of intrinsic continuum slopes, to investigate the dust reddening properties in these absorption systems we simulate the dust-reddened quasar spectrum using template quasar spectra. The templates include the average SDSS quasar composite spectrum from Vanden Berk et al. (2001), and the reddest-quartile and bluest-quartile composites from Richards et al. (2003) (composite spectra of SDSS quasars binned by continuum color). We adopt different types of extinction laws and treat $E(B - V)$, the amount of extinction, as a free parameter. We adopt the $E(\lambda - V)/E(B - V)$ relations from Pei

(1992) to calculate empirical extinction curves for the Milky Way, LMC and SMC. We also consider the “CCM Galactic extinction law” (Cardelli, Clayton & Mathis 1989), which gives a parameterized analytical form of $A(\lambda)/A(V)$ for wavelengths $\lambda > 1000 \text{ \AA}$:

$$\frac{A(\lambda)}{A(V)} = a(x) + \frac{b(x)}{R_V}$$

where $a(x)$ and $b(x)$ are uniquely defined curves as a function of the wavenumber $x = \lambda^{-1}$, and $R_V \equiv A(V)/E(B - V)$. (Note that the Milky Way empirical extinction curve used in Pei (1992) is equivalent to the CCM extinction law with $R_V = 3.08$, the mean value from measurements along different lines of sight.) These extinction curves are then applied to redden the template spectrum.

The simulated spectra are normalized to the data using the mean flux density between 7000–7500 \AA or 7500–8000 \AA in the observed frame, since the red end of each spectrum is least affected by dust extinction. The reduced χ^2 is calculated for each fit using the entire spectrum except for the emission line wavelength regions as defined in Vanden Berk et al. (2001) and for the wavelengths of narrow absorption lines.

We now discuss the fitting results for the three individual quasars. Table 1 lists the redshifts of the quasars and of all absorption lines identified in the intervening systems associated with the putative 2175 \AA bumps. The narrow absorption line parameters were measured using the IRAF² standard software package *splot*. We assume that all dust along the line of sight is located at these intervening redshifts. For clarity, all the fitting attempts with different quasar composite spectra are summarized in Table 2; all the 2175 \AA measurements and the metallicity estimates for three absorption systems are summarized in Table 3.

3.1. SDSS J1459+0024

The quasar redshift is $z = 3.0124 \pm 0.0005$, and a strong intervening absorption system is seen at $z = 1.3946 \pm 0.0001$ (all absorption redshifts are measured from the Mg II doublet). The broad absorption feature centered between the Ly α 1215 and C IV 1550 emission lines is consistent with being the 2175 \AA extinction feature from dust in the intervening absorption system at $z = 1.3946$. The restframe width of the broad absorption feature is $\sim 400 \pm 60 \text{ \AA}$

²IRAF is distributed by the National Optical Astronomy Observatories, which are operated by the Association of Universities for Research in Astronomy, Inc., under cooperative agreement with the National Science Foundation.

FWHM, and its central wavelength is $2230 \pm 20 \text{ \AA}$ at a redshift of $z = 1.395$. The measurements of FWHM and central wavelength are obtained with a Drude-like profile fit of the observed absorption feature³ (the same measurements for §3.2 and §3.3). The 1σ error is estimated by including different regions of continuum bracketing the feature into the fit (i.e., fit for several wavelength ranges between 2050–2550 \AA , in the dust restframe.). In the Milky Way this feature is observed to have an almost constant central wavelength $\lambda_0 = 2175 \pm 9 \text{ \AA}$. This central wavelength difference between the Milky Way and this absorption system likely arises from the uncertainty caused by the N v 1240 and Si iv 1398 emission lines bracketing the absorption feature. We rule out identifying this feature as a C iv broad absorption line trough because there is no evidence for broad absorption in other lines commonly seen in BAL quasars (e.g., N v).

By varying $E(B - V)$ with the Milky Way, LMC and SMC empirical curves, it is found that the best fit to both the broad absorption feature and the large scale reddening is obtained using a Milky Way-type extinction curve with $E(B - V) = 0.2$. The 2175 \AA bump in the simulated spectra reddened with the LMC or SMC curves is not sufficiently deep to match the bump in the observed spectrum, indicating the existence of Milky Way-type dust in this absorber. To find a better fit to the flux level and the overall shape of the broad absorption, we add in R_V as another free parameter by adopting the CCM extinction law. With the CCM extinction law, the best fit is obtained with the reddest composite, which gives $E(B - V) = 0.13 \pm 0.01$, $R_V = 1.9^{+0.3}_{-0.2}$ and a minimum reduced $\chi^2 \sim 1.8$. The 1σ error bar is estimated by variation of χ^2 . With the average and the bluest composite, we can still obtain a good overall fitting with slightly larger χ^2 (Table 2, Fig. 2). The fitting with composite spectra of different colors indicates $0.7 \lesssim R_V \lesssim 1.9$; the rather small value of R_V compared to the average value of 3.1 in the Milky Way (Savage & Mathis 1979) indicates that the size distribution of the dust grains is skewed towards substantially finer particles.⁴

Note that SDSS J1459+0024 is the only one of our three quasars detected by 2MASS, and its $J - K$ color of 1.22 ± 0.17 places it in the reddest quartile of $z = 3$ quasars (Barkhouse & Hall 2001). The dust in the intervening galaxy would not have much of an effect at the rest-frame wavelengths probed by the J and K bands, so the red $J - K$ color of SDSS J1459+0024 is good evidence that its UV-optical continuum is intrinsically red. This is

³The CCM functional form used a Drude-like profile to represent the 2175 \AA extinction hump: $\sim x^2 / [(x^2 - x_0^2)^2 + \gamma^2 x^2]$, $x \equiv \lambda^{-1}$, $x_0 = \lambda_0^{-1}$, where λ_0 is the central wavelength and γ is the FWHM. x_0 and γ are determined by fitting the observed spectrum (Fitzpatrick & Massa 1986; Cardelli, Clayton, & Mathis 1989).

⁴Although the exact R_V value is dependent on the adopted composite spectrum type (reddest, average, or bluest), it is somewhat secure to conclude that this absorber system favors smaller R_V (than that of the Milky Way) and the SMC-type extinction curve without the 2175 \AA hump is not able to give a good fit.

consistent with our result that the best fit is obtained with the reddest quartile composite.

3.2. SDSS J1446+0351

The quasar redshift is $z = 1.9452 \pm 0.0023$, and a strong intervening absorption system is seen at $z = 1.5115 \pm 0.0002$. Only a few absorption lines are identified in this absorption system, as listed in Table 1. The quasar spectrum shows a broad absorption feature centered between the C IV 1550 and C II] 2326 emission lines, consistent with the 2175 Å extinction feature from dust in the intervening absorption system at $z = 1.51$. The width of the broad absorption feature is $\sim 450 \pm 55$ Å FWHM, and its central wavelength is 2200 ± 15 Å at a redshift of $z = 1.51$. This small wavelength shift is probably due to the uncertainty produced by the C III] 1909 line superposed on the absorption feature.

With $E(B - V) = 0.28$ we obtain the best fit of the broad absorption feature and the large scale reddening with the empirical Milky Way-type extinction curve. Again, the 2175 Å absorption in the simulated spectra based on LMC and SMC curves is not deep enough to match the observations. With the CCM extinction law, we obtain the best fit using the reddest composite with $E(B - V) = 0.14 \pm 0.01$, $R_V = 0.7^{+0.4}_{-0.2}$ and a minimum reduced $\chi^2 \sim 2.6$. Using the average and the bluest composite, we obtained almost identical curves to the best fit with reddest composite and $0.5 \lesssim R_V \lesssim 0.7$ (Table 2, Fig. 3). This implies our fitting is not sensitive to the intrinsic quasar spectrum and the unexpected small value of R_V is not an artifact. The dust grain size distribution in this system also appears to be skewed towards smaller particles.

3.3. SDSS J0121+0027

The quasar redshift is $z = 2.2241 \pm 0.0001$, and a strong intervening absorption system is seen at $z = 1.3880 \pm 0.0001$. Standard lines identified in this absorption system are also listed in Table 1. Two other absorption systems are also seen in the spectrum: C IV, Si IV and possibly weak Mg II absorption at $z = 1.955 \pm 0.001$, and C IV, probably N V and possibly Ly α absorption at $z = 2.200 \pm 0.005$. Again the quasar spectrum shows a broad absorption feature, centered between the C IV 1550 Å and C III] 1909 Å emission lines, consistent with being the 2175 Å feature from dust in the $z = 1.388$ intervening absorption system. The central wavelength in the rest frame for the broad absorption feature is 2250 ± 25 Å and the restframe width is $\sim 400 \pm 60$ Å FWHM at a redshift of $z = 1.388$. The C IV emission probably causes the apparent shift of the dust absorption feature toward longer wavelengths

than seen in the Milky Way.

Using the Vanden Berk (2001) SDSS composite spectrum and simply varying $E(B - V)$ with the empirical curves, one cannot achieve a satisfactory overall fit to this quasar’s spectrum. With the bluest-quartile composite spectrum from Richards et al. (2003) and $E(B - V) = 0.14$, we obtain the best fit of the broad absorption feature and the large scale reddening using the Milky Way empirical extinction. With the LMC and SMC empirical extinction curves, the 2175 Å absorption is not sufficient to match the observed amplitude, also indicating Galactic-type dust content in this absorber (Fig. 4).

We applied the CCM Galactic extinction law to the same bluest-quartile composite. We obtain the best fit with $E(B - V) = 0.23^{+0.02}_{-0.01}$, $R_V = 5.5 \pm 0.1$ and a minimum reduced $\chi^2 \sim 1.3$ (Fig. 4). Using the reddest composite of Richards et al. (2003) leads to difficulty matching the flux in the far-UV region. We estimate a range of $5.5 \lesssim R_V \lesssim 6.0$ from the fitting results using the average and bluest composite (Table 2). The large value of R_V for this system implies that large dust grains are more prevalent than in the Milky Way diffuse ISM.

3.4. Discussion

The best fit parameters of both of the first two systems (SDSS J1459+0024 and SDSS 1446+0351) include surprisingly small R_V values, implying a relative overabundance of finer dust grains compared to Milky Way dust.⁵ In the Milky Way, so far the most extreme extinction curve is found for the line of sight toward the HD 210121 high latitude translucent cloud. The extinction curve, with $R_V \approx 2.1$, is characterized by an extremely steep far-UV rise and by a relatively weak and broader 2175 Å hump (Welty & Fowler 1992; Larson, Whittet, & Hough 1996). Detailed extinction, polarization and IR emission modeling implies that this region is rich in finer dust grains (Li & Greenberg 1998; Larson et al. 2000; Weingartner & Draine 2001; Clayton et al. 2003). Detailed modeling of the extinction curves of these intervening systems in terms of the silicate/graphite-PAHs model (Li & Draine 2001) are in progress (J.Wang et al. 2004, in preparation). Our goal is to infer their dust size distribution and composition. However, there are other possible explanations. For example, if the quasars are intrinsically redder than indicated by our fits, to reproduce their observed far-UV spectra would require extinction curves which are less steep in the far ultraviolet (i.e., which have higher R_V). We note that there are also uncertainties in the 5–6 μm^{-1} range of

⁵The previously reported minimum $R_V = 1.5$ is associated with an elliptical galaxy at $z = 0.96$ (Falco et al. 1999).

the CCM extinction curve.

Nonetheless, since the physical conditions governing dust properties evolve with redshift (e.g., star formation rate, metallicity, etc.), it should not be surprising that the dust properties also evolve with redshift. If the diversity of grain sizes is real and not due to biases in the extinction modeling (in both our work and that of other groups mentioned in §1), it is extremely interesting for understanding dust formation at high redshift. Generally speaking, preferential removal of small dust grains (e.g. by coagulation in dense molecular clouds) will result in a gray extinction law with large R_V , while in star forming galaxies finer grains will dominate the dust size distribution as a result of dust destruction by grain-grain collisions or grain shattering by shock waves.

Lack of the detailed knowledge of the metallicity of these absorber systems, we use the Milky Way gas-to-dust ratios $N(\text{H I}+\text{H}_2)/E(B-V) = 5.8 \times 10^{21} \text{ cm}^{-2} \text{ mag}^{-1}$ (Bohlin, Savage, & Drake 1978) and $N(\text{H I})/E(B-V) = 4.93 \pm 0.28 \times 10^{21} \text{ cm}^{-2} \text{ mag}^{-1}$ (Diplas & Savage 1994) to estimate the neutral gas content of these absorption systems. From our best fit $E(B-V)$ values we estimate $N(\text{H I}) \approx 6.4 \times 10^{20} \text{ cm}^{-2}$ for SDSS J1459+0024 and $N(\text{H I}) \approx 6.9 \times 10^{20} \text{ cm}^{-2}$ for SDSS J1446+0351. The strength of the Mg II absorptions suggest that those absorbers may be damped Ly α systems, which have a lower limit to their column densities of $N(\text{H I}) = 2 \times 10^{20} \text{ cm}^{-2}$. From the SDSS spectra of the two quasars (spectral resolution ~ 2000), the equivalent width ratio of Mg II $\lambda\lambda 2796, 2803$ indicates that both lines are either saturated or nearly so. Therefore we can constrain the range of column densities for Mg II: $7.7 \times 10^{13} \leq N(\text{Mg II}) \leq 3.1 \times 10^{17} \text{ cm}^{-2}$ for SDSS J1459+0024 and $1.7 \times 10^{14} \leq N(\text{Mg II}) \leq 7.0 \times 10^{17} \text{ cm}^{-2}$ for SDSS J1446+0351. The lower and upper ends of these ranges represent the linear and damping regimes of Mg II, respectively. A lower limit estimate of the Mg II abundance compared to solar abundance gives $[\text{Mg}/\text{H}] = -2.7$ for SDSS J1459+0024 and $[\text{Mg}/\text{H}] = -2.2$ for SDSS J1446+0351. No Zn II lines were found in either system, so we cannot estimate the dust depletion. Some recent surveys have discovered strong molecular hydrogen lines in damped Ly α absorbers with strong dust depletion, suggesting that the formation of H_2 on the dust grains is the dominant formation process (Ge & Bechtold 1997, 1999; Ge, Bechtold & Kulkarni 2001). HST observations of these quasars will be extremely valuable to verify this hypothesis.

For SDSS J0121+0027, using the Milky Way gas-to-dust ratio we estimate an average hydrogen column density $N(\text{H I}) \approx 1.1 \times 10^{21} \text{ cm}^{-2}$ from our best fit $E(B-V) = 0.23$. Again, this suggests that the strong Mg II absorption system is a damped Ly α absorption system. Based on the equivalent widths of the weak absorption lines of Zn II 2026 and Fe II 2587 in the $z = 1.388$ absorber, we estimate the column densities for Zn II and Fe II are $3.4 \times 10^{13} \text{ cm}^{-2}$ and $1.6 \times 10^{14} \text{ cm}^{-2}$, respectively, assuming they are both on the linear part of the curve

of growth. Since both Zn II and Fe II are the dominant species for these metals in DLAs, the estimated Zn and Fe abundances are $[\text{Zn}/\text{H}] \simeq -0.2$ and $[\text{Fe}/\text{H}] \simeq -2.6$, respectively. The relative depletion between Fe and Zn, $[\text{Fe}/\text{Zn}] \sim -2.4$, is very large, similar to heavily depleted diffuse clouds in the Milky Way, such as the ζ Oph cloud ($[\text{Fe}/\text{Zn}] \simeq -1.6$, Savage & Sembach 1996). This dust depletion is the largest among all of the high-redshift DLAs searched for dust and molecular absorption to date (Ge, Bechtold & Kulkarni 2001; Ledoux, Petitjean, & Srianand 2003). The large dust depletion provides additional evidence that the strong dust extinction feature in this system is real.

Although the precise nature of the carrier of the 2175 Å extinction feature remains unknown, it is generally accepted that this feature arises in some types of aromatic carbonaceous materials (Draine 2003; Li & Greenberg 2003). A proposal involving a cosmic mixture of many individual PAH molecules, radicals, and ions is receiving increasing attention (Li & Draine 2001). PAHs, the most abundant and widespread organic molecules in the Milky Way Galaxy as well as in other nearby galaxies (Allamandola & Hudgins 2003), reveal their existence in interstellar space by emitting a distinctive set of broad spectral lines at 3.3, 6.2, 7.7, 8.6 and 11.3 μm (Li & Draine 2001). PAHs are thought to form predominantly in the atmospheres of carbon stars (Latter 1991; Allain, Leach & Sedlmayr 1996); from there, stellar winds will deposit PAHs into the surrounding ISM.⁶ As the single largest repository of organic material in our galaxy, PAHs play an important role in prebiotic chemistry which may ultimately lead to the development of organic life. Under dense molecular cloud conditions, energetic processing (starlight irradiation and/or cosmic ray bombardment) of ices containing PAHs produces aromatic alcohols, ethers, ketones, and quinones; these are essential for important processes in living systems (Bernstein et al. 1999, 2002, 2003). Such complex organic molecules can be delivered to the surfaces of planetary objects via dust particles (Clemett et al. 1999) and carbonaceous meteorites (Zenobi, Philippoz, Zare, & Buseck 1989) — the formation mechanism of complex organic molecules found in such meteorites is not known for certain, but the deuterium enrichment seen in many such molecules suggests an interstellar origin (Cronin et al. 1993).

The presence of PAHs in distant galaxies may thus be of astrobiological interest. The galactic environments in the galaxies discussed in this paper have probably evolved to the

⁶We should note that the origin and evolution of interstellar PAHs are not very clear. Other suggested sources for interstellar PAHs include (1) shattering of carbonaceous interstellar dust or of photoprocessed interstellar dust organic mantles (Greenberg et al. 2000) by grain-grain collisions in interstellar shocks (Jones, Tielens, & Hollenbach 1996); (2) *in-situ* formation through ion-molecule reactions (Herbst 1991). In the early universe, massive rate of star formation results in a much denser UV starlight intensity and a much greater supernova explosion rate. Both effects would enhance the destruction of PAHs. We would admit that even the origin and survival of PAHs in the Milky Way galaxy are not well understood. See Li (2004) for details.

stage where the above-mentioned organic molecules, and possibly even molecules of ribonucleic acid and of various proteins, can form on the surfaces of dust consisting of PAHs (Bernstein et al. 2002; Muñoz Caro et al. 2002). If this is the case, then the building blocks of life may have been present billions of years before the formation of the Earth.

4. Conclusion

We report three direct spectroscopic detections of the 2175 Å dust absorption feature in quasar absorption systems at redshifts $1.4 \lesssim z \lesssim 1.5$. These are the first detections of this feature in individual Mg II absorption systems. From fitting the composite SDSS quasar spectra reddened by a CCM Galactic extinction law to the observed spectra, we derive best-fit reddening parameters $E(B - V) \approx 0.14$, $R_V \approx 0.7$ for SDSS J1446+0351, $E(B - V) \approx 0.13$, $R_V \approx 1.9$ for SDSS J1459+0024 and $E(B - V) \approx 0.23$, $R_V \approx 5.5$ for SDSS J0121+0027. The various R_V values in these systems compared to the average Galactic value of $R_V = 3.1$ indicates a wide range of dominant grain sizes among intervening absorption systems. We found that although the intrinsic slope of the quasar continuum in each system is unknown, we can still meaningfully constrain the R_V value in each system. If the presently favored PAH model for the 2175 Å feature carrier is correct, we have detected complex organic molecules in the young universe, about 9 billion years ago. The presence of PAHs at such large lookback times may be of astrobiological interest.

J. W. and J. G. acknowledge support from NSF grant AST-01-38235, AST-02-43090 and NASA grants NAG 5-12115, and NAG 5-11427. P. B. H. acknowledges support from the Department of Astrophysical Sciences at Princeton University. D. P. S. acknowledges NSF grant NSF03-007582. We thank the referee for his useful comments and suggestions. Funding for the creation and distribution of the SDSS Archive has been provided by the Alfred P. Sloan Foundation, the Participating Institutions, the National Aeronautics and Space Administration, the National Science Foundation, the U.S. Department of Energy, the Japanese Monbukagakusho, and the Max Planck Society. The SDSS Web site is <http://www.sdss.org/>. The SDSS is managed by the Astrophysical Research Consortium (ARC) for the Participating Institutions. The Participating Institutions are The University of Chicago, Fermilab, the Institute for Advanced Study, the Japan Participation Group, The Johns Hopkins University, Los Alamos National Laboratory, the Max-Planck-Institute for Astronomy (MPIA), the Max-Planck-Institute for Astrophysics (MPA), New Mexico State University, University of Pittsburgh, Princeton University, the United States Naval Observatory, and the University of Washington.

REFERENCES

- Abazajian, K. et al. 2003, *AJ*, 126, 2081
- Allain, T., Leach, S. & Sedlmayr, E. 1996, *A&A*, 305, 602
- Allamandola, L. J., & Hudgins, D. M. 2003, in *Solid State Astrochemistry*, ed. V. Pirronello, J. Krelowski, & G. Manicó (Dordrecht: Kluwer), 251
- Barkhouse, W. A. & Hall, P. B. 2001, *AJ*, 121, 2843
- Bernstein, M. P., Elsila, J. E., Dworkin, J. P., Sandford, S. A., Allamandola, L. J., & Zare, R. N. 2002, *ApJ*, 576, 1115
- Bernstein, M. P., Moore, M. H., Elsila, J. E., Sandford, S. A., Allamandola, L. J., & Zare, R. N. 2003, *ApJ*, 582, L25
- Bernstein, M. P., Sandford, S. A., Allamandola, L. J., Gillette, J. S., Clemett, S. J., & Zare, R. N. 1999, *Science*, 283, 1135
- Bernstein, M. P., Dworkin, J. P., Sandford, S. A., Cooper, G. W., & Allamandola, L. J. 2002, *Nature*, 416, 401
- Blanton, M. R. et al. 2003, *ApJ*, 594, 186
- Bohlin, R. C., Savage, B. D., & Drake, J. F. 1978, *ApJ*, 224, 291
- Cardelli, J. A., Clayton, G. C., & Mathis, J. S. 1989, *ApJ*, 345, 245
- Clayton, G. C., Wolff, M. J., Sofia, U. J., Gordon, K. D., & Misselt, K. A. 2003, *ApJ*, 588, 871
- Clemett, S. J., Maechling, C. R., Zare, R. N., Swan, P. D., & Walker, R. M. 1993, *Science*, 262, 721
- Cohen, R. D., Burbidge, E. M., Junkkarinen, V. T., Lyons, R. W., & Madejski, G. 1999, *BAAS*, 31, 942
- Cronin, J. R., Pizzarello, S., Epstein, S., & Krishnamurthy, R. V. 1993, *Geochim. Cosmochim. Acta*, 57, 4745
- Diplas, A. & Savage, B. D. 1994, *ApJ*, 427, 274
- Draine, B. T. 2003, *ARA&A*, 41, 241

- Falco, E. E. et al. 1999, *ApJ*, 523, 617
- Fitzpatrick, E. L. & Massa, D. 1986, *ApJ*, 307, 286
- Fukugita, M., et al. 1996, *AJ*, 111, 1748
- Ge, J. & Bechtold, J. 1997, *ApJ*, 477, L73
- Ge, J. & Bechtold, J. 1999, in *ASP Conf. Ser. 156, Highly Redshifted Radio Lines*, ed. C. L. Carilli, S. J. E. Radford, K. M. Menten, & G. I. Langston (San Francisco: ASP), 121
- Ge, J., Bechtold, J. & Kulkarni, V. P. 2001, *ApJ*, 547, L1
- Greenberg, J. M., et al. 2000, *ApJ*, 531, L71
- Gunn, J. E., et al. 1998, *AJ*, 116, 3040
- Hall, P. B., Hopkins, P., Strauss, M., Richards, G. & Brinkmann, J. 2004, to appear in “AGN Physics with the Sloan Digital Sky Survey,” ed. G. T. Richards & P. B. Hall (astro-ph/0312281)
- Herbst, E. 1991, *ApJ*, 366, 133
- Joblin, C., Leger, A., & Martin, P. 1992, *ApJ*, 393, L79
- Jones, A. P., Tielens, A. G. G. M., & Hollenbach, D. J. 1996, *ApJ*, 469, 740
- Larson, K. A., Whittet, D. C. B., & Hough, J. H. 1996, *ApJ*, 472, 755
- Larson, K. A., Wolff, M. J., Roberge, W. G., Whittet, D. C. B., & He, L. 2000, *ApJ*, 532, 1021
- Latter, W.B. 1991, *ApJ*, 377, 187
- Ledoux, C., Petitjean, P., & Srianand, R. 2003, *MNRAS*, 346, 209
- Li, A. 2004, in *ASP Conf. Ser. 309, Astrophysics of Dust*, ed. A.N. Witt, G.C. Clayton, & B.T. Draine (San Francisco: ASP), 417
- Li, A., & Draine, B. T. 2001, *ApJ*, 554, 778
- Li, A. & Greenberg, J. M. 1998, *A&A*, 339, 591
- Li, A., & Greenberg, J.M. 2003, in *Solid State Astrochemistry*, ed. V. Pirronello, J. Krelowski, & G. Manicó (Dordrecht: Kluwer), 37

- Malhotra, S. 1997, *ApJ*, 488, L101
- Morton, D. C. 1991, *ApJS*, 77, 119
- Motta, V. et al. 2002, *ApJ*, 574, 719
- Muñoz, J. A., Falco, E. E., Kochanek, C. S., McLeod, B. A., & Mediavilla, E. 2004, *ApJ*, in press (astro-ph/0401548)
- Muñoz Caro, G. M., et al. 2002, *Nature*, 416, 403
- Pei, Y. C. 1992, *ApJ*, 395, 130
- Pier, J. R., et al. 2003, *AJ*, 125, 1559
- Pitman, K. M., Clayton, G. C., & Gordon, K. D. 2000, *PASP*, 112, 537
- Richards, G. T., et al. 2002, *AJ*, 123, 2945
- Richards, G. T. et al. 2003, *AJ*, 126, 1131
- Savage, B. D. & Mathis, J. S. 1979, *ARA&A*, 17, 73
- Savage, B. D. & Sembach, K. R. 1996, *ARA&A*, 34, 279
- Schneider, D. P. et al. 2003, 126, 2579
- Stecher, T. P. 1965, *ApJ*, 142, 1683
- Strauss, M. A., et al. 2002, *AJ*, 124, 1810
- Toft, S., Hjorth, J., & Burud, I. 2000, *A&A*, 357, 115
- Vanden Berk, D. E., et al. 2001, *AJ*, 122, 549
- Vernet, J., et al. 2001, *A&A*, 366, 7
- Weingartner, J. C. & Draine, B. T. 2001, *ApJ*, 548, 296
- Welty, D. E. & Fowler, J. R. 1992, *ApJ*, 393, 193
- Wucknitz, O., Wisotzki, L., Lopez, S., & Gregg, M. D. 2003, *A&A*, 405, 445
- York, D. G., et al. 2000, *AJ*, 120, 1579
- Zenobi, R., Philippos, J., Zare, R. N., & Buseck, P. R. 1989, *Science*, 246, 1026

Table 1. Strong lines identified in dusty intervening absorption systems

$\lambda_{\text{rest}}(\text{\AA})$	Ion	$\lambda_{\text{obs}}(\text{\AA})$	$EW_{\text{rest}} \pm 1\sigma \text{ error}(\text{\AA})$	f	z
SDSS J1459+0024 $z_Q = 3.0124$					
2852.9642	MgI	6830.6	0.50 ± 0.04	1.81	1.3942
2803.531	MgII	6713.6	1.67 ± 0.04	0.295	1.3947
2796.352	MgII	6695.7	1.96 ± 0.04	0.592	1.3945
2600.1729	FeII	6226.4	0.92 ± 0.08	0.203	1.3946
2586.6500	FeII	6194.6	0.58 ± 0.17	0.0573	1.3947
2382.7652	FeII	5705.6	1.09 ± 0.12	0.328	1.3946
2344.2139	FeII	5613.0	0.50 ± 0.04	0.108	1.3945
1670.7874	AlIII	4003.8	4.97 ± 0.88	1.88	1.3959
SDSS J1446+0351 $z_Q = 1.9452$					
2803.531	MgII	7022.5	3.66 ± 0.24	0.295	1.5113
2796.352	MgII	7041.8	4.50 ± 0.20	0.592	1.5117
2600.1729	FeII	6532.5	2.31 ± 0.12	0.203	1.5120
1670.7874	AlIII	4196.03	0.96 ± 0.12	1.88	1.5114
SDSS J0121+0027 $z_Q = 2.2241$					
2852.9642	MgI	6814.0	0.92 ± 0.08	1.81	1.3884
2803.531	MgII	6695.0	2.72 ± 0.08	0.295	1.3881
2796.352	MgII	6677.4	3.52 ± 0.08	0.592	1.3879
2600.1729	FeII	6209.2	1.84 ± 0.13	0.203	1.3880
2586.6500	FeII	6176.2	0.54 ± 0.04	0.0573	1.3877
2344.2139	FeII	5597.7	1.05 ± 0.17	0.108	1.3879
2026.137	ZnII	4836.6	0.50 ± 0.04	0.412	1.3871
1862.7895	AlIII	4448.8	0.50 ± 0.08	0.268	1.3882
1854.7164	AlIII	4430.2	1.05 ± 0.13	0.539	1.3886
1808.0126	SiII	4309.2	0.75 ± 0.08	0.0055	1.3834
1670.7874	AlIII	3989.6	1.13 ± 0.08	1.88	1.3879

Note. — Vacuum wavelengths, oscillator strength f are from Morton (1991). Equivalent width is measured in the absorber restframe.

Table 2. Fitting log with CCM extinction curve using different composite spectra

Composite used	$[R_V, E(B - V)]$	Reduced χ^2
SDSS J1459+0024		
Reddest	[1.9, 0.13]	1.8
Average	[0.7, 0.14]	2.0
Bluest	[0.7, 0.14]	2.0
SDSS J1446+0351		
Reddest	[0.7, 0.15]	2.6
Average	[0.5, 0.16]	3.0
Bluest	[0.6, 0.18]	2.9
SDSS J0121+0027		
Reddest	[6.0, 0.17]	5.8
Average	[6.0, 0.23]	2.5
Bluest	[5.5, 0.23]	1.3

Note. — “Reddest” and “Bluest” refer to the reddest and bluest quartile composite quasar spectrum from Richards et al. (2003). “Average” refers to the composite quasar spectrum using median combining from Vanden Berk et al. (2001).

Table 3. Summary of the 2175 Å measurements and metallicity estimates for three sightlines

Line-of-sight	z_{abs}	$\lambda_0(\text{\AA})^a$	FWHM(Å) ^b	$N(\text{H I}) \text{ (cm}^{-2}\text{)}^c$	$[\text{X/H}]^d$
SDSS J1459+0024	1.3946	2230±20	400±60	6.4×10^{20}	$[\text{Mg/H}] \simeq -2.7$
SDSS J1446+0351	1.5115	2200±15	450±55	6.9×10^{20}	$[\text{Mg/H}] \simeq -2.2$
SDSS J0121+0027	1.3880	2250±25	400±60	1.1×10^{21}	$[\text{Zn/H}] \simeq -0.2; [\text{Fe/H}] \simeq -2.6$

^aCentral wavelength of the 2175 Å feature.

^bFull Width Half Maximum of the 2175 Å feature.

^cEstimated H I column density in the absorption system along line-of-sight.

^dEstimated metallicity $[\text{X/H}] \equiv \log(\text{X/H}) - \log(\text{X/H})_{\odot}$ in the absorption system. Reference solar abundances are from Savage & Sembach (1996).

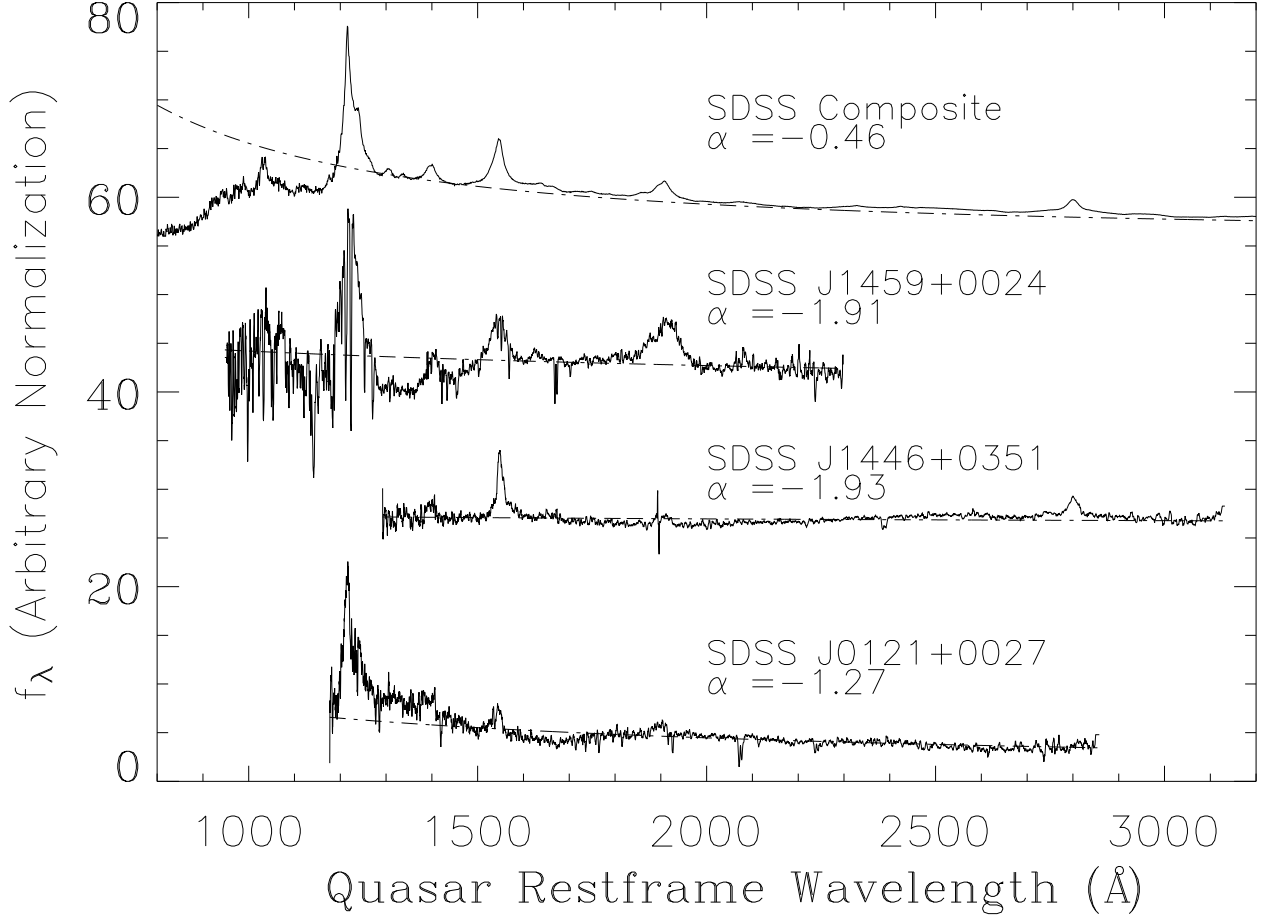


Fig. 1.— Comparison between the composite quasar spectrum from Vanden Berk et al. (2001) (top; spectral index $\alpha = -0.46$), the observed spectrum of SDSS J1459+0024 (second from top; spectral index $\alpha = -1.91$), the observed spectrum of SDSS J1446+0351 (third from top; spectral index $\alpha = -1.93$) and the observed spectrum of SDSS J0121+0027 (bottom; spectral index $\alpha = -1.27$). Power law fits to estimated continuum flux are shown as the dashed lines. The broad absorption features at ~ 1400 Å in the quasar SDSS J1459+0024 restframe, at ~ 1900 Å in the quasar SDSS J1446+0351 restframe and at ~ 1700 Å in the quasar SDSS J0121+0027 restframe are identified as the 2175 Å dust extinction feature.

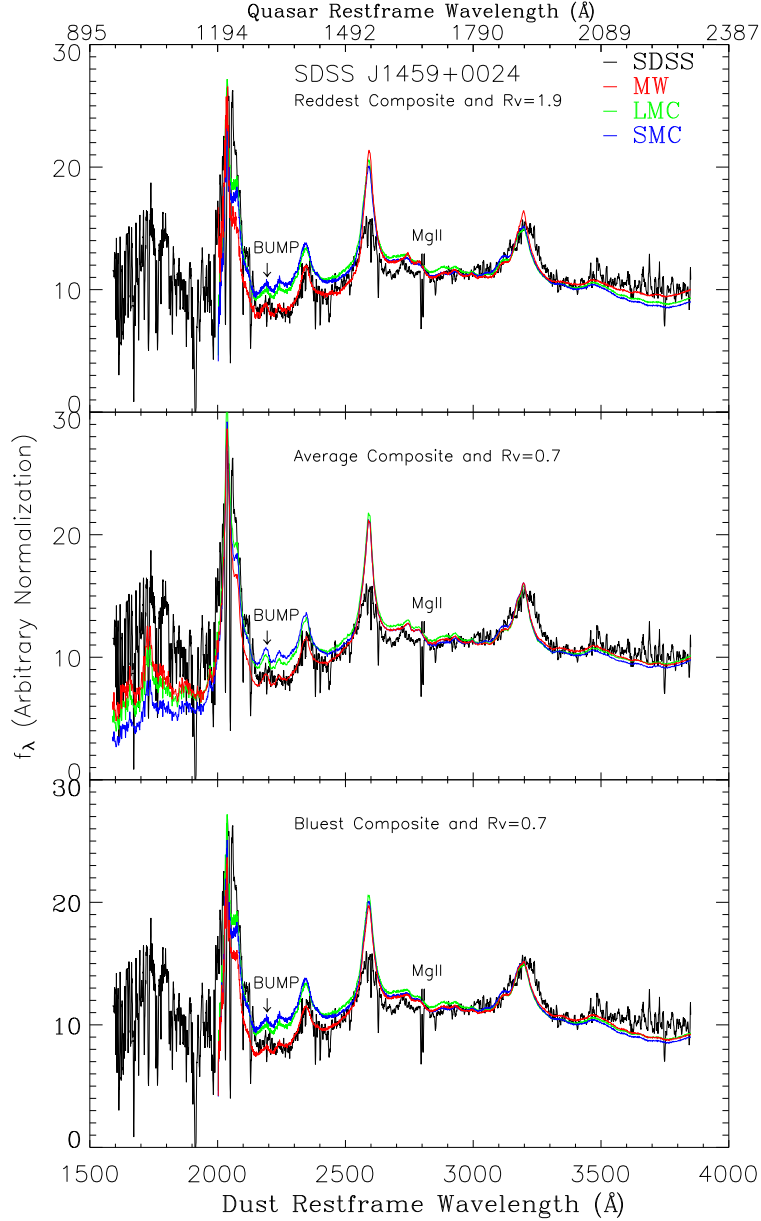


Fig. 2.— Comparison of the observed SDSS J1459+0024 spectrum (black) with model spectra obtained by reddening the SDSS composite quasar spectrum (top panel: the reddest quartile composite from Richards et al. (2003); middle panel: average composite from Vanden Berk et al. (2001); bottom panel: the bluest quartile composite from Richards et al. (2003)) with three types of extinction curves: Milky Way with various R_V (red), LMC (green), SMC (blue). All spectra are normalized so that they have equal flux density at 3200 Å. The model spectra using the composite from Richards et al. (2003) can not cover the entire observed spectrum simply because the bluest end of the composite starts from ~ 1195 Å. The best fit is obtained using the reddest quartile composite, reddened by a Milky Way-type extinction curve with $R_V \approx 1.9$.

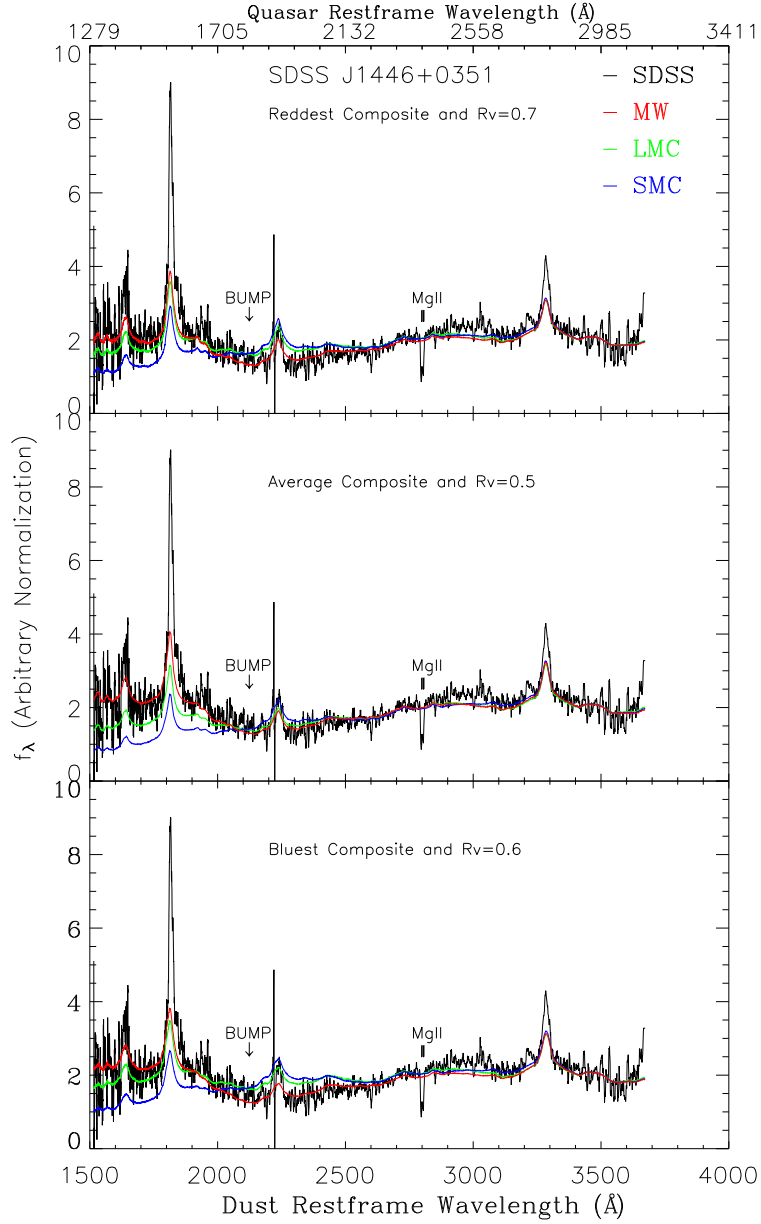


Fig. 3.— Comparison of the observed SDSS J1446+0351 spectrum (black) with model spectra same as Fig. 2 but for SDSS J1446+0351. All spectra are normalized so that they have equal flux density at 3400 Å. The best fit is obtained using the reddest quartile composite, reddened by a Milky Way-type extinction curve with $R_V \approx 0.7$.

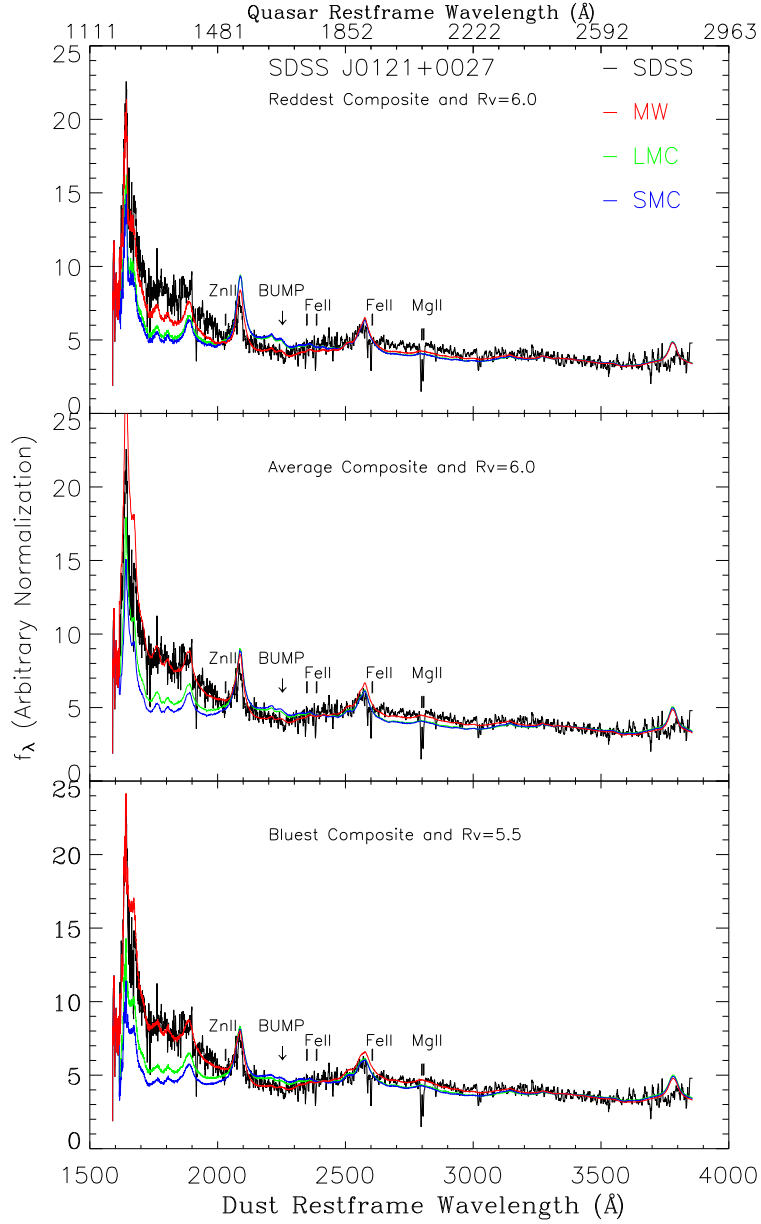


Fig. 4.— Comparison of the observed SDSS J0121+0027 spectrum (black) with model spectra same as Fig. 2 but for SDSS J0121+0027. All spectra are normalized so that they have equal flux density at 3300 Å. The best fit is obtained using the bluest quartile composite, reddened by a Milky Way-type extinction curve with $R_V \approx 5.5$.